Thermophysics and Aeromechanics, *2014*, *Vol. 21*, *No. 6*

Boundary-layer structure in the flow around the cellular surface in a flat channel*

V.I. Terekhov[1,2], Ya.I. Smulsky[1], K.A. Sharov[1], and A.V. Zolotukhin[2]

[1]*Kutateladze Institute of Thermophysics SB RAS*, *Novosibirsk*, *Russia*

[2]*Novosibirsk State Technical University*, *Novosibirsk*, *Russia*

E-mail: terekhov@itp.nsc.ru

(*Received September 2*, *2014*; *in revised form September 9*, *2014*)

The results of experimental study of the turbulent flow structure at longitudinal flow around the cellular surface with hexagonal cells of 5-mm size, 21-mm depth and wall thickness of 0.2 mm are presented. The measurements were performed using the PIV system for the developed flow in the channel with cross section of 21×150 mm and length of 1000 mm. Stroboscopic visualization of the flow was performed, and velocity and turbulence components were measured in the channel with and without the cells. It is shown that in a vicinity of cells, the boundary layer is less filled, but it has the higher level of turbulent fluctuations. It is noted that in contrast to the profile on a smooth wall there is no logarithmic region on the cellular surface. In this case, there are no effects of velocity slip on the cellular surface under the experimental conditions.

Key words: boundary layer**,** cellular surface, turbulence, method of digital tracer visualization, tracers, hexagonal cells.

Introduction

One of priorities of the modern aerohydrodynamics and heat transfer theory is the search for the new methods of heat transfer intensification at parity or even reduced growth of hydraulic losses. In this respect, the surfaces with alveolar reliefs, which recently attract much interest, are illustrative [1, 2]. Some experimental and numerical studies in this area show high potential of these methods, which can lead to improved thermal-hydraulic characteristics. A variety of ways to reduce hydraulic losses (riblets [3], longitudinal destroyers of large vortices [4] as well as vortex-acoustic generators like Helmholtz resonators [5, 6]) is of great interest both in terms of physical foundations of these devices with a complex mechanism for formation of turbulent flow field near the wall, and from the viewpoint of their practical use. The detailed review of the current state of methods for surface friction reduction can be found in some works [7, 8].

The considered cellular surfaces used, in particular, for the purposes of thermal protection of spacecraft elements have some similar features with the above mentioned vortex generators. This is proved by the results of the first experimental studies of longitudinal flow around the surfaces with cellular coatings [9–12]. The main feature of the aerodynamic pattern of flow

* The work was financially supported by the Russian Science Foundation (Grant No. 14-19-00402).

interaction with the cells is the effect of the flow slip on the wall, whose value can reach up to 30 % of the velocity in the flow core. This fact and data on friction reduction by means of acoustic damping [13] provide a basis for the use of such systems of vortex generators as the efficient methods of control of turbulent transfer. A lack of detailed experimental data on the flow field structure does not allow the construction of a complete picture of this complex phenomenon and requires deeper investigation.

This research deals with experimental investigation of development of the flow field and turbulent characteristics along the surface with hexagonal cells. Data on the averaged and turbulent characteristics of the cellular surface and channel with smooth walls are directly compared in the present study.

1. Experimental setup and measurement methods

The working channel of experimental setup had the rectangular cross section of 21 × × 150 mm, length of 1 m, and it was made of transparent organic glass with the thickness of 8 mm. The transverse dimensions of the inlet channel were selected under the condition of two-dimensional flow in the central longitudinal section of the channel. At the distance of 580 mm from the channel inlet, a plate of 40×200 mm with hexagonal cells was mounted (Fig. 1). The cellular surface was mounted to put the edges of the open part of a cell at one level with the surface of the working channel wall. The opposite side of the cellular surface was closed by a textolite plate. The depth of the cells was 21 mm, they were made of textolite with the wall thickness of 0.2 mm. The typical cell sizes are indicated on the right of Fig. 1. The long side of the plate with cells was oriented along the flow, and it was arranged symmetrical relative to the axis of the wide side of a flat channel. The distance to the lateral walls was 55 mm. The light sheet through the upper translucent lid cut the flow along the axis of the wide side of the channel and fell on the cellular surface; coordinate x was measured along the flow, and the coordinate y was measured from the cell surface opposite wall.

The experimental setup includes all elements of the wind tunnel required for generation of a high-quality flow: settling chamber, nozzle and working channel. In the current experiments, we studied the developed flow along the length of the cellular plate at the constant Reynolds number $\mathrm{Re} = Uh/\nu = 2.1 \cdot 10^4$; at the entrance of the cellular plate, the flow was developed.

The PIV system consisting of the pulsed Nd:YAG laser of 90-mJ power with the wavelength of 532.05 nm and flash duration of 5 ns and the digital camera with 1-Mpix matrix were used for measurements. The laser sheet was generated in the midsection of the channel by means of a special optic insert, and its thickness was 3 mm. The digital camera allowed the paired frames with frequency of 3 Hz and minimal gap between the frames of 20 ms. The water fog particles with the size of 1 μm, generated by the Safex fog-generator of DANTEC production were used as the tracers. Fog was fed to the inlet of setup compressor. The measurement region, covered by the camera with the help of "Industar" object-glass and extension rings, was 17×20 mm. The depth of field was individual for each experiment because the optics was adjusted depending on the kind of illumination afforded by the wall, which in turn was determined by the manner how the cells are captured: the side, front or rear walls. The ratio of channel height to its width was relatively high (~1/7), therefore, a core, extended along the transverse coordinate, was formed in the middle part of the channel. The flow in this core was almost two-dimensional. This core and insignificant

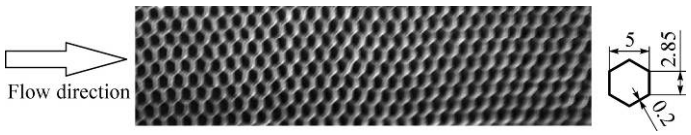

Fig. 1. Cellular section and sizes (sizes are in mm).

changes in velocity along the channel width were registered during the special tests when measuring the corresponding profiles along the channel width.

During the measurements, there were up to three cells in the frame. This area was divided into smaller computational domains, where the velocity vectors were calculated. In calculations, we used the cross-correlation Fourier method with the iterative algorithm. The size of computational domain was 32×32 pixels with a scale factor of 15 μm/pix. Considering the 50-% overlap region, the minimal distance from the wall, where the measurement was made, was ~0.3 mm. After calculation of the vector field, the vectors were filtered by the signal/noise ratio using the median filter. After screening the vectors, the vector field was interpolated, then, the averaged and statistical characteristics were calculated. The sampling set in experiments was 4000 vector fields.

2. Experimental results and discussion

The profiles of longitudinal velocity, longitudinal and transverse pulsations, and shear stresses in the smooth and cellular channels are compared in Fig. 2. All data there were obtained for the cross section located at $x/h = 6.5$ from the beginning of the cellular section.

According to data presented, the flow near the cellular surface differs absolutely from the flow around a smooth wall. Near the cellular surface, the velocity profile is less flat in comparison with the classical distribution on a smooth wall (Fig. 2*a*). We should note that longitudinal and transverse velocity fluctuations (Figs. 2*b* and 2*c*, respectively) near the cellular surface are much higher than those on the smooth surface. This tendency is also typical of shear stress distributions across the channel (Fig. 2*d*). In the channel with smooth walls, as was expected, the shear stress distribution along the height is linear, but in the channel with cells at distance $y/h \sim 0.2$, the stresses increase more than by the factor of three.

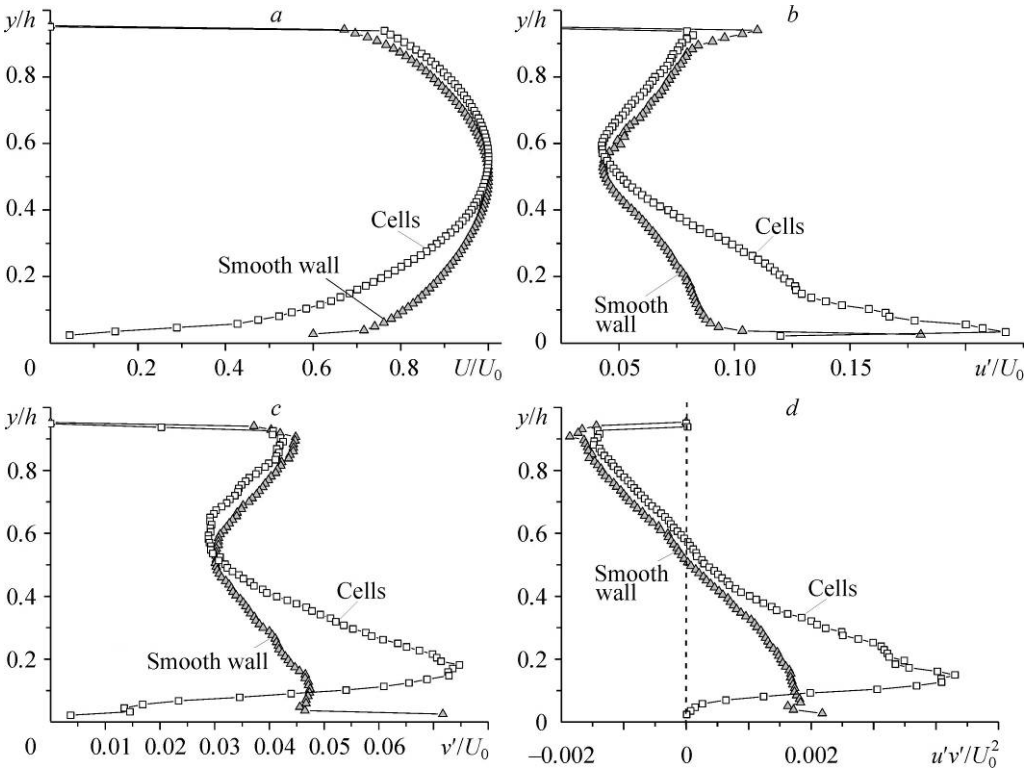

Fig. 2. Distribution of longitudinal velocity (*a*), longitudinal (*b*) and transverse (*c*) fluctuations, and shear stresses (*d*) along the channel height; $x/h = 6.5$.

Simultaneously, the stable tendency to reduction of transverse velocity fluctuations and turbulent shear stresses is observed near the walls.

Such a complex scenario of flow development is caused by interaction of the boundary layer with the cells. Actually, the flow around the holes of various shapes (cylindrical cavity [14], craters [15], transverse groove [16], etc.) on the surface leads to formation of a periodic vortex layer behind them. However, we failed to discover such structures in the current research, perhaps, because of relatively small sizes of cells.

Development of longitudinal velocity profiles in the boundary layer on the cellular surface is shown in Fig. 3. Distributions in the developed turbulent and laminar boundary layers are shown there as the limiting dependences. Experimental data for the smooth wall are in good agreement with the power velocity law: $n = 1/7$. On the cellular surface, the boundary layer is pushed away from the wall, and then with its further motion, the deformed region extends to the larger part of the boundary layer. As a result, the profile becomes less filled and approaches the profile characteristic to the laminar flow. In this case, as was shown by measurements, near the cellular surface there is almost no region with logarithmic law of velocity distribution. This can be concluded from Fig. 4, which shows that the greatest changes in the boundary layer, blowing up the cellular surface, start in a buffer area, and its outer part remains conservative to a change in the boundary conditions on the surface. The dynamic velocity for all cross sections on the cellular surface was calculated by relations for a flat wall. We should note also that the friction coefficient for smooth channel found by the Clauser method corresponds to the value calculated for the classical turbulent boundary layer [17]. According to the data in Fig. 4, it is impossible to determine in this way the friction resistance on the cellular surface.

One of fundamental differences between the results obtained and experimental data of work [9–11] is an absence of flow slip along the cellular surface, which, according to these data, could reach about 20–30% of the velocity in the flow core. This result should be also checked on the cells of other sizes with varying Reynolds number in the channel.

Distributions of the form parameter of the boundary layer $H = \delta^*/\delta^{**}$ and integral Reynolds number Re^{**} along the cellular surface is shown in Fig. 5. Coordinate $x/h = 0$ corresponds to the beginning of the cellular region. Before this region, the value of H corresponds to the developed turbulent layer; then, its increase to the value typical of the laminar flow ($H \to 2.7$), and following decrease are observed. This behavior of the form parameter is caused by the fact that the velocity profile becomes sloping with simultaneously increasing turbulence and shear stresses. The Reynolds number of momentum thickness changes in the same manner with development of the flow above the cellular surface: it increases first and then decreases. Now it is impossible to formulate the reasons for such a behavior of local and integral characteristics of the turbulent flow around the surface with cells because of multifactor nature and complexity of the aerodynamic structure. This problem requires subsequent detailed studies.

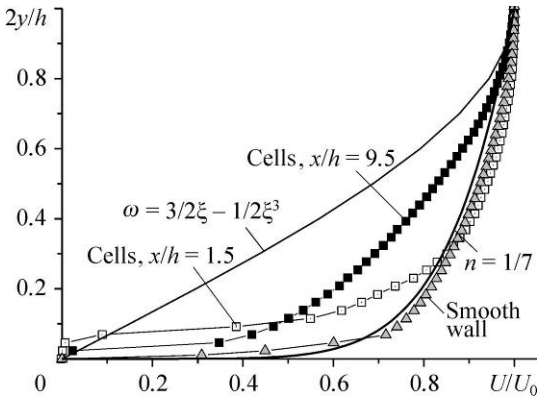

Fig. 3. Comparison of velocity profiles on the smooth and cellular surfaces.

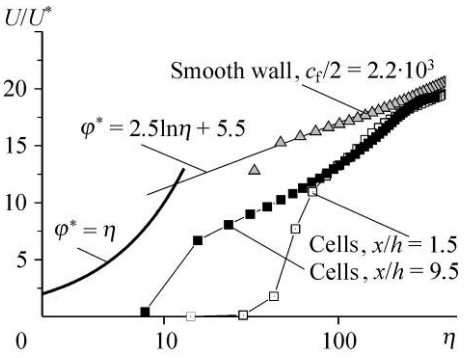

Fig. 4. Profiles of longitudinal velocity on the smooth and cellular surfaces in universal coordinates.

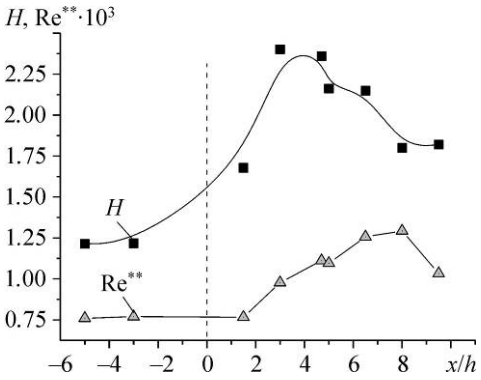

Fig. 5. A change in the form parameter H and integral Reynolds number along the cellular surface.

Conclusions

Results of experimental studies of the averaged flow, normal and tangential stresses at the flow around the cellular surface with the typical cell size of ~ 5 mm are presented. The measurements were performed using the two-component PIV system. The flow was organized in a flat channel of 21×150×1000 mm.

It was found that the boundary layer on the cellular surface is less filled in comparison with the smooth wall at simultaneous growth of turbulent fluctuations and shear stresses. There is almost no logarithmic region in velocity distribution, and the effect of flow slide relative to the cellular surface is not observed.

Nomenclature

f — frequency, Hz,
h — channel height, m,
$H = \delta^*/\delta^{**}$ — form parameter of boundary layer,
x, y — longitudinal and transverse coordinates, m,
U_0 — maximal longitudinal velocity, m/s,
U, V — longitudinal and transverse velocity components, m/s,
$\mathrm{Re} = Uh/\nu$, $\mathrm{Re}^{**} = U\delta^{**}/\nu$ — Reynolds numbers,
v^* — dynamic velocity, m/s,
δ^*, δ^{**} — displacement and momentum thicknesses, m,
ν — dynamic viscosity, m^2/s,
u', v', $u'v'$ — axial and transverse pulsations (m/s) and Reynolds stresses (m^2/s^2).

References

1. **S.A. Isaev, N.V. Kornev, A.I. Leontiev, and E. Hassel,** Influence of the Reynolds number and the spherical dimple depth on the turbulent heat transfer and hydraulic loss in a narrow channel, Int. J. Heat Mass Transfer, 2010, Vol. 53, P. 178–197.
2. **G.V. Kovalenko, V.I. Terekhov, and A.A. Khalatov,** Flow regimes in a single dimple on the channel surface, J. Appl. Mech. Tech. Phys., 2010, Vol. 51, No. 6, P. 839–848.
3. **G.R. Grek, V. Kozlov, and S. Titarenko,** An experimental study of the influence of riblets on transition, J. Fluid Mech., 1996, Vol. 315, P. 31–49.
4. **R.K. Shah and A.M. Jacobi,** Heat transfer surface enhancement through the use of longitudinal vortices: a review of recent progress, Exp. Thermal and Fluid Sci., 1995, Vol. 11, No. 3, P. 295–309.
5. **R.L. Panton, P. Kevin, K.P. Flynn, and D.G. Bogard,** Control of turbulence through a row on Helmholtz resonators, AIAA Paper, 1987, No. 87-0436.
6. **N.N. Kovalnogov and L.V. Khakhaleva,** The motion and friction resistance of a turbulent flow in a perforated tube with damping cavities, Izv. VUZ. Aviatsionnaya Tekhnika, 2002, No. 3. P. 19–21.

7. **Y.M. Chung and T. Talha,** Effectiveness of active flow control for turbulent skin friction drag reduction, Physics of Fluids, 2011, Vol. 23, No. 2, 025102.
8. **V.I. Kornilov,** Reduction of turbulent friction by active and passive methods (Review), Thermophysics and Aeromechanics, 2005, Vol. 12, No. 2, P. 175–196.
9. **A.A. Klimov and S.A. Trdatyan,** The use of a honeycomb surface for controlling the boundary layer, High Temperature, 2003, Vol. 41, No. 6, P. 801–806.
10. **S.A. Trdatyan and A.A. Klimov,** Friction and heat transfer on a honeycomb surface in laminar and turbulent flows, in: Proc. 12th Int. Heat Transfer Conf., Grenoble, 2002, P. 221.
11. **S.A. Trdatyan and A.A. Klimov,** A boundary layer on the honeycomb surface at inleakage of the laminar flow, P.2. Forced convection of the single-phase liquid, in: Proc. 3d Russian National Conference on Heat and Mass Transfer, MEI, Moscow, 2002, P. 281–284.
12. **U. Butt,** Experimental investigation of the flow over macroscopic hexagonal structured surfaces, Von der Fakultät für Maschinenbau, Elektrotechnik und Wirtschaftsingenieurwesen der Brandenburgischen Technischen Universität Cottbus-Senftenberg zur Erlangung des akademischen Grades eines Doktor-Ingenieurs genehmigte Dissertation, Brandenburg, April 2014.
13. **N.N. Kovalnogov,** The model of turbulent transfer in a boundary layer on the perforated surface with tight damping cavities, Izv. VUZ. Problemy energetiki, 2003, No. 5–6, P. 41–47.
14. **M. Hiwada, T. Kawamura, J. Mabuchi, and M. Kumada,** Some characteristics of flow pattern and heat transfer past a circular cylindrical cavity, Bull. JSME, 1983, Vol. 26, No. 220, P. 1744–1752.
15. **V.I. Terekhov, S. V. Kalinina, and Yu.M. Mshvidobadze,** Experimental study of flow development in the channel with a semispherical cavity, Sibirsk. fiziko-tekhn. zhurnal, 1992, No. 1, P. 77–85.
16. **V.I. Terekhov, N.I. Yarygina, and A.V. Shaporin,** Heat transfer in three-dimensional separated flow in a rectangular cavity, Industrial Heat Transfer, 1999, Vol. 21, No. 2–3, P. 22–25.
17. **S.S. Kutateladze and A.I. Leontiev,** Heat Transfer, Mass Transfer and Friction in Turbulent Boundary Layers, Hemisphere Publishing Corporation, 1989.